Quaternary Structures of Intermediately Ligated Human Hemoglobin A and Influences from Strong Allosteric Effectors: Resonance Raman Investigation

Shigenori Nagatomo,* Masako Nagai,† Yasuhisa Mizutani,‡ Takashi Yonetani,§ and Teizo Kitagawa*

*Okazaki Institute for Integrative Bioscience, National Institutes of Natural Sciences, Myodaiji, Okazaki, Aichi, Japan; †Department of Material Chemistry, Faculty of Engineering, Hosei University, Koganei, Tokyo, Japan; ‡Molecular Photoscience Research Center, Kobe University, Kobe, Hyogo, Japan; and §Department of Biochemistry and Biophysics, University of Pennsylvania, School of Medicine, Philadelphia, Pennsylvania

ABSTRACT The Fe-histidine stretching ($\nu_{Fe\text{-}His}$) frequency was determined for deoxy subunits of intermediately ligated human hemoglobin A in equilibrium and CO-photodissociated picosecond transient species in the presence and absence of strong allosteric effectors like inositol(hexakis)phosphate, bezafibrate, and 2,3-bisphosphoglycerate. The $\nu_{Fe\text{-}His}$ frequency of deoxyHb A was unaltered by the effectors. The T-to-R transition occurred around $m = 2$–3 in the absence of effectors but $m > 3.5$ in their presence, where m is the average number of ligands bound to Hb and was determined from the intensity of the ν_4 band measured in the same experiment. The $\alpha 1$-$\beta 2$ subunit contacts revealed by ultraviolet resonance Raman spectra, which were distinctly different between the T and R states, remained unchanged by the effectors. This observation would solve the recent discrepancy that the strong effectors remove the cooperativity of oxygen binding in the low-affinity limit, whereas the ^{1}H NMR spectrum of fully ligated form exhibits the pattern of the R state.

INTRODUCTION

Human hemoglobin A (Hb A) with α_2-β_2 tetramer structure, exhibiting positive cooperativity in oxygen binding, has been extensively investigated with various methods, since it serves as a basic model for general allosteric proteins (1), and currently, elucidation of a structural mechanism of cooperativity is a major subject of Hb studies. X-ray crystallographic studies have demonstrated the presence of two distinct quaternary structures, called T (tense) and R (relaxed) states, which correspond to the low- and high-affinity states, respectively, and whose typical structures are practically seen for the deoxy and CO-bound forms of Hb A, respectively (2,3). The cooperative oxygen binding of Hb has been explained in terms of a reversible transition between the two quaternary structures, switching of which takes place at a certain number of bound ligands (4,5,6). However, recent, more extensive examinations in the presence of various allosteric effectors like 2,3-bisphosphoglycerate (BPG), inositol(hexakis)phosphate (IHP), and bezafibrate (BZF) at a wide range of pH stressed importance of the tertiary structure change for oxygen affinity rather than the quaternary structure (7), demonstrating that the T/R two-state model is applicable only within a single set of oxygen binding equilibria.

To correlate the cooperativity with a structure, it seems to be indispensable to acknowledge the presence of some plasticity within each of the T and R quaternary structures when the T and R are used (8). In addition, there would be synergistic effects between specific interactions at the central cavity and other sites (9). Thus, the structural characterization of Hb in terms of T and R is insufficient. This is partially due to the neglect of the differences between the α and β subunits in the simplified two-state model. Nevertheless, the idea of the T/R structures seems to hold some essence of Hb cooperativity. Here, we examined whether the Raman spectral changes of Hb caused by BPG, IHP, and BZF are explicable in the framework of the two-state model or not.

Phosphate ions of BPG and IHP are indeed working in animal red cells (10,11) to adjust oxygen affinity, whereas BZF is widely used to take care of high fat diseases (12). These effectors do not affect oxygen affinity of proteins like myoglobin (Mb) and isolated chains of Hb A. Thus, some specific subunit contacts are indispensable for these effectors to alter oxygen affinity of Hb, even if the tertiary structure is essential to oxygen affinity. It is premised that appreciable tertiary-structure changes are always accompanied by a change of quaternary state and their extents are different between the α and β subunits. In the case of the simple two-state model, x-ray crystallographic analysis (13) indicated that the largest structural differences between the T and R states are present at the $\alpha 1$-$\beta 2$ subunit interface, where resets of hydrogen bonds and salt bridges take place upon ligand binding to deoxyHb. In ^{1}H NMR spectroscopy Tyrα42, which forms a hydrogen bond with Aspβ99 in the T state, and thus yields a well-defined peak, becomes free in the R state, and therefore the peak apparently disappears due to rapid exchanges. This ^{1}H signal has served as a diagnostic marker for the quaternary structure (14,15). However, Yonetani et al.

Submitted November 1, 2004, and accepted for publication May 3, 2005.

Address reprint requests to Teizo Kitagawa, Okazaki Institute for Integrative Bioscience, National Institutes of Natural Sciences, Myodaiji, Okazaki, Aichi 444-8787, Japan. Tel.: 81-564-59-5225; Fax: 81-564-59-5229; E-mail: teizo@ims.ac.jp.

Shigenori Nagatomo's present address is Graduate School of Pure and Applied Sciences, University of Tsukuba, Tsukuba, Ibaraki 305-8571, Japan.

0006-3495/05/08/1203/11 $2.00

doi: 10.1529/biophysj.104.049775

observed the disappearance of this ^{1}H NMR signal for the fully ligated Hb A in the presence of BZF and IHP despite the fact that Hb A in this solution condition exhibits extremely low oxygen affinity and no cooperativity (7), thus seeming to be frozen in the T state even after being fully ligated. It is also found recently (16) that BZF binds to the globin near the E-helix of the α subunit, which is distinct from the binding of IHP and BPG to the central cavity at an intersubunit space between the two β subunits. Due to their different binding sites, additivity of the effects are understandable when IHP and BZF are present at the same time, but it became desirable to reexamine the relations among the quaternary structure, tertiary structure, oxygen affinity, and cooperativity.

A practical question to be answered is whether the ordinary quaternary-structure change occurs to Hb A in the process of oxygen binding when both BZF and IHP are present at pH 6.4, for which there is apparently no cooperativity. If the fully ligated form adopts the R structure, as indicated by the ^{1}H NMR study, but its oxygen binding is not cooperative, then a quaternary structure would not be directly related to the oxygen affinity and its change may not be essential to cooperativity. This would lead to overthrow the well-established interpretation of Hb cooperativity in terms of the two-state model (2–6).

It is in general agreement that the strain in the Fe-His bond, monitored by visible resonance Raman (RR) spectroscopy, is one of the main factors to determine the oxygen affinity for human Hb A (17), and that some changes at the subunit contacts are substantial for of cooperativity to occur (4,5,18,19). The α1-β2 intersubunit contacts induce some strain on the Fe-His bond of deoxy heme, which lowers the Fe-His stretching ($\nu_{\text{Fe-His}}$) frequency, but its appearance differs between the α and β subunits. Magnitude of the strain in the Fe-His bond is much larger for the α than the β subunit. On the other hand, the globin structures in the T and R states of Hb A can be diagnosed by vibrational spectra of the interacting residues, which can be evaluated by (UVRR) resonance Raman spectroscopy (20,21). Therefore, to explore structural influences of strong allosteric effectors, we applied some new techniques of RR spectroscopy to the quaternary structure changes of Hb A upon ligand dissociation. Here we focused on intermediately ligand-bound states ($m \neq 0$ or 4, m is the number of ligands bound to Hb), which are practically difficult to generate with ordinary static techniques but can be explored with dynamical techniques like time-resolved measurements for photolysed CO-bound Hb A (COHb), in which the average m number in a photo-steady-state between photolysis and geminate recombination is varied by variation of a laser power and determined with intensity of the ν_4 band.

MATERIALS AND METHODS

Materials

HbA was purified from fresh human blood by a preparative isoelectric focusing electrophoresis (Amersham Biosciences, Uppsala, Sweden) (20,22); ~150 μL of the 200-μM (in terms of heme) Hb A solution was put into a spinning cell made of a synthetic quartz EPR tube (diameter, 5 mm) (23). DeoxyHb and COHb were prepared by adding sodium dithionite (1 mg/mL) to oxyHb after replacement of the inside air of the sample tube with N_2 and CO, respectively. Five typical conditions of solvents, characterized in Table 1, were selected for comparison: 1), pH 9, no effector; 2), pH 7.4, 5 mM BPG; 3), pH 6.4, 5 mM BZF; 4), pH 6.4, 5 mM IHP; and 5), pH 6.6, 1 mM BZF and 5 mM IHP. Influences of an allosteric effector are expected to become progressively stronger from condition 1 to 5. Solvents used were 0.05 M HEPES buffer for all the pH range (pH 6.4–9.0), and a pH value in the presence of a selected allosteric effector was determined for a solution in the Raman cell with a pH meter (Φ720, Beckman Coulter, Fullerton, CA).

Visible resonance Raman measurements

Visible resonance Raman spectra were excited with the 441.6-nm line of a He/Cd laser (Kimmon Electrics, Tokyo, Japan) and detected with a liquid nitrogen-cooled charge coupled device (Princeton Instruments, Tucson, AZ), attached to a home-designed 100-cm single polychromator (Ritsu Oyo Kogaku, Saitama, Japan) (24). The slit width and slit height were set at 150 μm and 20 mm, respectively, and the wavenumber-width per one channel of the detector was 0.7 cm^{-1}. The laser power used was 5.4 mW for deoxyHb and 0.065–11 mW for COHb at the sample point for steady-state measurements. The fully deoxy form was measured with a constant-rate (1000-rpm) spinning cell at an ambient temperature, whereas intermediately ligated forms of COHb were measured with a variable-rate spinning cell (180, 600, and 1800 rpm were adopted) with a diameter of 4.5 mm. Raman shifts were calibrated with indene or carbon tetrachloride, and the accuracy of the peak position of well-defined Raman bands was $\pm$1 cm^{-1}.

Ultraviolet resonance Raman measurements

UVRR spectra were excited by a XeCl excimer (LPX120I) laser-pumped dye laser (SCANMATE, Lambda Physik, Göttingen, Germany). The 308-nm line from the XeCl excimer laser (operated at 100 Hz) served as a pump to excite coumarin-480 in the dye laser, and its 470-nm output was frequency-doubled with a β-BaB_2O_4 crystal to generate 235-nm pulses. Details of the measurement system were described in a previous work (25).

Time-resolved resonance Raman measurements

Picosecond time-resolved RR spectra were obtained using a homemade pump/probe system, in which wavelengths of the probe and pump beams were set to be 442 and 540 nm, respectively. Details of apparatus were described previously (26–28).

RESULTS

Structural dependences on allosteric effectors in fully deoxy- and fully CO-bound forms of Hb

Fig. 1 shows the 441.6-nm excited RR spectra of deoxyHb A in the presence of 0.5 mM BZF and 2 mM IHP at pH 6.3 (*A*),

TABLE 1 Solution conditions, oxygen affinity, and cooperativity for five samples

Number	Solution conditions	K_T/torr^{-1}	K_R/torr^{-1}	n_{max}
1	pH 9, no effector	0.25	10	2.5
2	pH 7.4, 5 mM BPG	0.04	8	3.0
3	pH 6.4, 5 mM BZF	0.016	0.8	2.1
4	pH 6.4, 5 mM IHP	0.008	0.16	1.9
5	pH 6.6, 1 mM BZF + 5 mM IHP	0.006	0.02	1.3

The oxygen affinity and cooperativity are represented in terms of the association constant (K) and the Hill coefficient (n_{max}), respectively, and their values are transferred from Perutz (5). $K = [HbO_2]/[Hb][O_2]$.

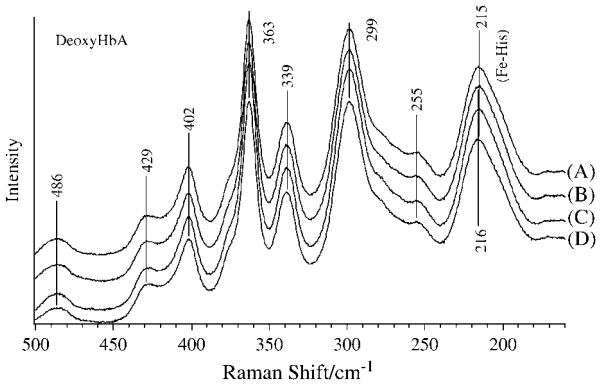

FIGURE 1 The 441.6-nm excited RR spectra of deoxyHb at pH 6.3 (BZF 0.5 mM and IHP 2 mM, *A*), at pH 6.3 (BZF 5mM, *B*), at pH 7.5 (BPG 2 mM, *C*), and at pH 8.9 (no effector, *D*). All samples are equilibrated with 0.05 M HEPES buffer, containing 0.1 M Na_2SO_4, and protein concentrations were 200 μM in heme. Laser power at the sample point was 2.1 mW and the spectra are the sum of 20 exposures of 60 s each.

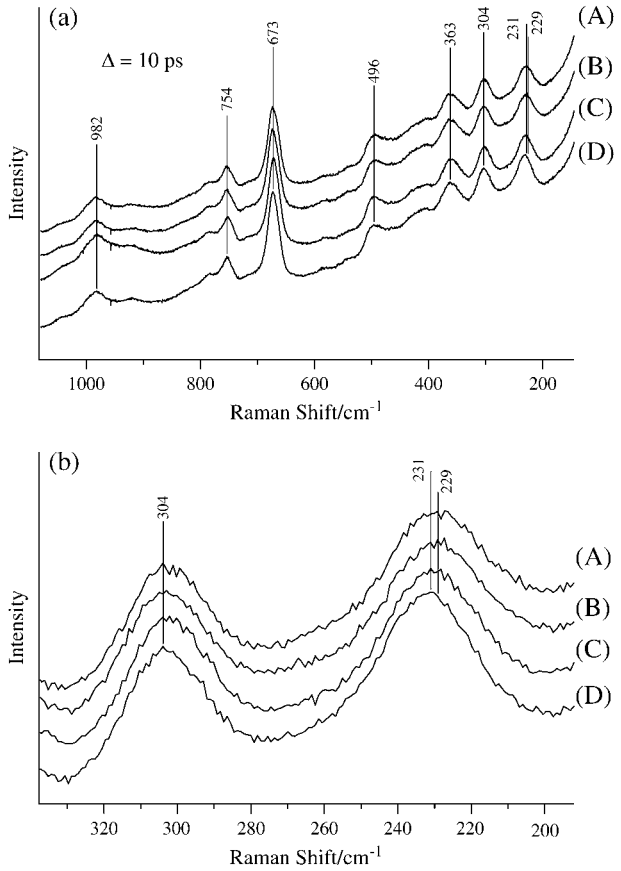

FIGURE 2 The 442-nm excited RR spectra at 10 ps after photodissociation of COHb upon pumping at 540 nm for the solution conditions of pH 6.5, with 0.75 mM BZF and 3 mM IHP (*A*), pH 6.5 with 7.5 mM BZF (*B*), pH 7.4 with 3 mM BPG (*C*), and pH 8.8 with no effectors (*D*). All samples are equilibrated with 0.05 M HEPES buffer, containing 0.1 M Na_2SO_4, and protein concentrations were 300 μM in heme. Panel *a* shows the spectral region between 150 and 1050 cm^{-1},, whereas panel *b* shows their expansion for the frequency region between 190 and 330 cm^{-1}. The spectral contributions from nonphotodissociated species have been subtracted.

5 mM BZF at pH 6.3 (*B*), 2 mM BPG at pH 7.5 (*C*) and no effector at pH 8.9 (*D*). The oxygen affinity becomes higher by a factor of 41 within the category of T going from *A* to *D*. Nevertheless, the four RR spectra are very much alike. If the strain exerted by a globin on a heme is larger in the case of the low-affinity extreme, the Fe-histidine (F8) bond should involve the strain, and its stretching frequency should become lower. Unexpectedly, the quaternary structure-sensitive Fe-histidine stretching mode ($\nu_{\text{Fe-His}}$) observed around 215 cm^{-1} exhibits little difference (1 cm^{-1}). The value of $\nu_{\text{Fe-His}}$ (215 cm^{-1}) for *A* is typical among the T-state deoxy Hb A, indicating that even the combination of strong allosteric effectors, BZF + IHP, hardly changes the magnitude of strain imposed on the Fe-His bond of deoxy subunits. The vibrations involving the vinyl bending mode around 429 and 401 cm^{-1} and the propionate bending mode around 363 cm^{-1}, the assignments of which are based on Spiro and co-workers (29,30), yield practically the same frequencies for the four different conditions, meaning that the side-chain geometry is unaltered by the allosteric effectors.

Fig. 2 shows the photodissociated transient RR spectra of COHb A observed at 10 ps after photolysis of CO, in which the pump power was adjusted to photodissociate COHb at most 10% in one event and the probe power was set so low that it did not cause photodissociation at all. Although the $\nu_{\text{Fe-His}}$ mode has no Raman intensity for the CO-bound form, the photodissociated transient five-coordinate species exhibits time-dependent intensity change for the $\nu_{\text{Fe-His}}$ band. In the case of carbonmonoxy myoglobin (COMb), its intensity increases with time: 90% of the intensity change occurs within 1 ps, whereas the remaining 10% in 10–20 ps (26). This intensity increase matches with the time dependence of a band-center shift of the near-infrared charge-transfer band (31) and is considered to reflect the time dependence of the out-of-plane displacement of the Fe atom (32). On the other hand, the frequency shift of the $\nu_{\text{Fe-His}}$ mode of the transient deoxyMb takes place with a time constant of 100 ps, reflecting a tertiary structure change of globin (26,27) and its rate depends on the viscosity of solvent. The corresponding shift of the $\nu_{\text{Fe-His}}$ band for COHb takes place with a time constant of ~300 ps (33) and is distinguished from a quaternary structure-dependent larger frequency shift (34).

It is known that the relaxation of the $\nu_{\text{Fe-His}}$ frequency due to the quaternary-structure change is extremely slow for Hb (34,35). In fact, the $\nu_{\text{Fe-His}}$ frequency of the early transient species in the picosecond timescale is considerably higher than those for the equilibrium deoxy species, indicating the presence of unrelaxed five-coordinate deoxy heme with the Fe atom on the porphyrin plane. Due to this feature, the RR spectra shown in Fig. 2 *a* are appreciably different from the spectra in the equilibrium state shown in Fig. 1 representing

individual peak frequencies and intensities. The 982-cm^{-1} band in Fig. 2 *a* arises from SO_4^{2-} ions present commonly as an internal intensity standard. The 338-cm^{-1} band in Fig. 1, which was noted by Friedman to exhibit time-dependent intensity changes for COHb after photolysis (34), is absent in Fig. 2 *a*, although its structural meaning remains to be explored.

The $\nu_{Fe\text{-}His}$ frequency at 10 ps after photolysis is inferred to reflect some properties of the CO-bound form and, therefore, the $\nu_{Fe\text{-}His}$ spectral region is expanded in Fig. 2 *b*. The transient $\nu_{Fe\text{-}His}$ frequencies of all the four cases are indeed distinctly higher than those of equilibrium deoxyHb and differ little among solvent conditions; the highest is 231 cm^{-1} for *D*, which represents a typical R state in the CO-bound form, and the lowest is 229 cm^{-1} for *A*, which represents the lowest-affinity extreme, whereas the frequency of the out-of-plane skeletal deformation mode (γ_7) is identical, at 304 cm^{-1}, among the four conditions. Anyway, the maximum frequency difference of $\nu_{Fe\text{-}His}$ ($\Delta\nu = 2$ cm^{-1}), which would be due to differences in the magnitude of strain in the CO-bound forms, is much smaller than the general T/R frequency difference of deoxyHb (6 cm^{-1}) (36), as well as those between the unrelaxed and relaxed deoxyHbs (~15 cm^{-1}) (34,35). Consequently, we conclude that the heme structures of the CO-bound Hb A under these four different solvent conditions are substantially alike.

Fig. 3 shows the 235-nm excited UVRR spectra of deoxyHb A (*A* and *B*) under two typical solvent conditions (5 and 2) and the deoxyHb minus COHb difference spectra (*D*–*F*) for three solvent conditions (5, 4, and 2). Since BZF itself gives strong UVRR bands, whose spectrum is delineated by spectrum *C*, the contribution from BZF was subtracted from the spectrum observed for condition 5, and the resultant spectrum is represented as spectrum *A*. The deoxy-minus-CO difference spectrum for isolated α chains in the presence of IHP and BZF is also displayed as spectrum *G*, in which some features around 1600 cm^{-1} could not be canceled completely on account of effects of a strong band of BZF.

The UVRR spectra of Hb A contain mainly the bands of Trp and Tyr residues, which are designated in the figure by W and Y, respectively, followed by a mode number, and the vibrational assignments are based on the work of Harada and co-workers (37). The intensities of spectra *A* and *B* are normalized with the band of SO_4^{2-} ions at 980 cm^{-1}. Generally, the T/R quaternary structure differences are sensitively indicated by the UVRR bands of W3, W7, W16, W17, and W18 of Trp residues and Y8a, Y7a, and Y9a of Tyr residues (18–21,38–40). Although the difference peak intensities of spectrum *D* are larger than those of spectra *E* and *F*, this is partially caused by the subtraction procedure of the spectrum of BZF and therefore is ignored in this study. The spectral patterns remain unchanged among spectra (*D*–*F*). If a quite different globin structure is generated by the simultaneous presence of IHP and BZF, some bands of Tyr and Trp residues might be shifted and the spectral pattern would be altered. Since there was no appreciable difference among the spectra of their CO-bound forms under the conditions 2, 4, and 5, the small spectral differences between *D* and *E* (or *F*) are ascribed to the deoxy form. On the other hand, there are no clear difference peaks for isolated α chain in the presence of IHP and BZF. Accordingly, these UVRR difference spectra indicate that the T structures in the deoxy form are of similar type, at least regarding the $\alpha 1$-$\beta 2$ subunit contacts, but their interactions might be strongest for solution 5 and weakest for solution 2.

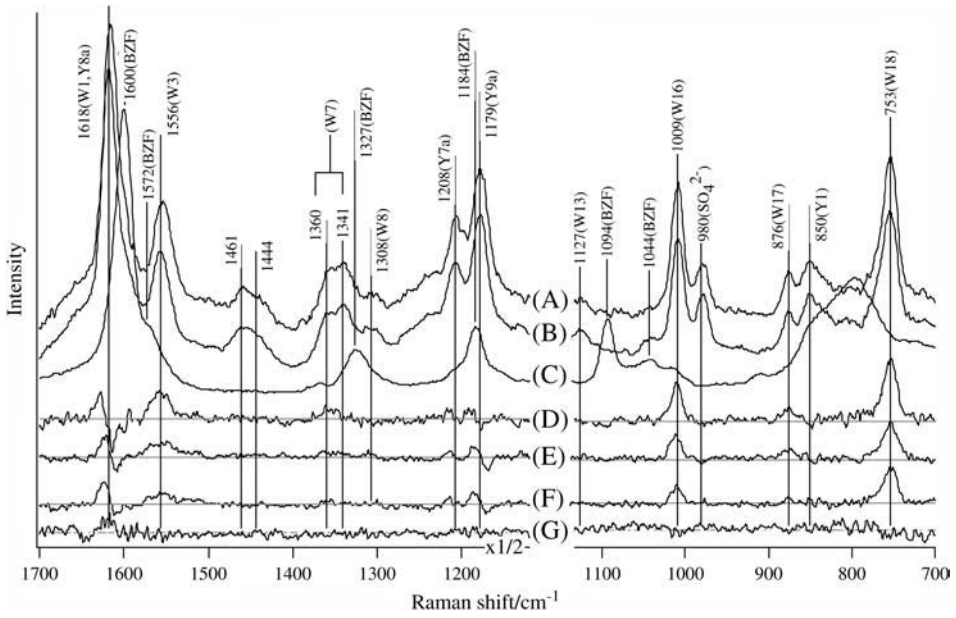

FIGURE 3 The 235-nm excited UVRR spectra of deoxyHbA at pH 6.6 with 1 mM BZF and 5 mM IHP (*A*), and at pH 7.5 with 5 mM BPG (*B*), and their respective deoxyHb-minus-COHb difference spectra. *D* and *F* are difference spectra for *A* and *B*, respectively, whereas *E* is the corresponding difference for the solution at pH 6.4 with 5 mM IHP and *G* denotes the corresponding difference of the isolated α chain in the presence of 5 mM IHP and 1 mM BZF. The 235-nm excited UVRR spectrum of BZF (1 mM) in the same buffer is also included as spectrum *C*. The assignments of bands are marked beside the wavenumber, in which Y and W denote the modes of Tyr and Trp residues, respectively. The band at 980 cm^{-1} arises from SO_4^{2-} ions contained as an internal intensity standard. All samples of Hb are equilibrated with 0.05 M HEPES buffer, containing 0.2 M Na_2SO_4, and the protein concentrations were 400 μM in heme.

Structural dependence on allosteric effectors in partially CO-bound forms of Hb

The amount of photodissociated species can be changed by laser power. Here, 100% and 50% photolysis mean that the numbers of CO molecules (m) remaining on Hb after photolysis of COHb are 0 and 2, respectively, on average. Fig. 4 explains how to determine m in the steady-state experiment. In this measurement, the probe light works also as a pump light; that is, a given molecule in the spinning cell encounters two photons during a single stay in the laser beam, in which the first photon (the pump photon) induces photodissociation of CO and the second photon (the probe photon) yields Raman scattering. Since the source is a CW laser, the photon flux is assumed to be not so high, as three or more photons interact with a given molecule in a single stay in the laser beam. The maximum delay time of the probe photon from the pump photon is the residence time of a molecule in the laser beam. Since the diameter of the irradiation beam is adjusted to be 0.5 mm, and the velocity (v mm/s) of a given molecule can be calculated from the spinning rate (p rpm) and diameter ($2d$ mm) of the cell to be $2dp\pi/60$, the residence time of the molecule in the laser beam is given by $0.5/v$ s. Thus, photodissociation and geminate recombination of CO are in photo-steady state while a molecule stays in the laser beam. In one turn of the cell ($60/p$ s), all the photodissociated deoxyHb molecules are recombined with CO under the present pressure of CO.

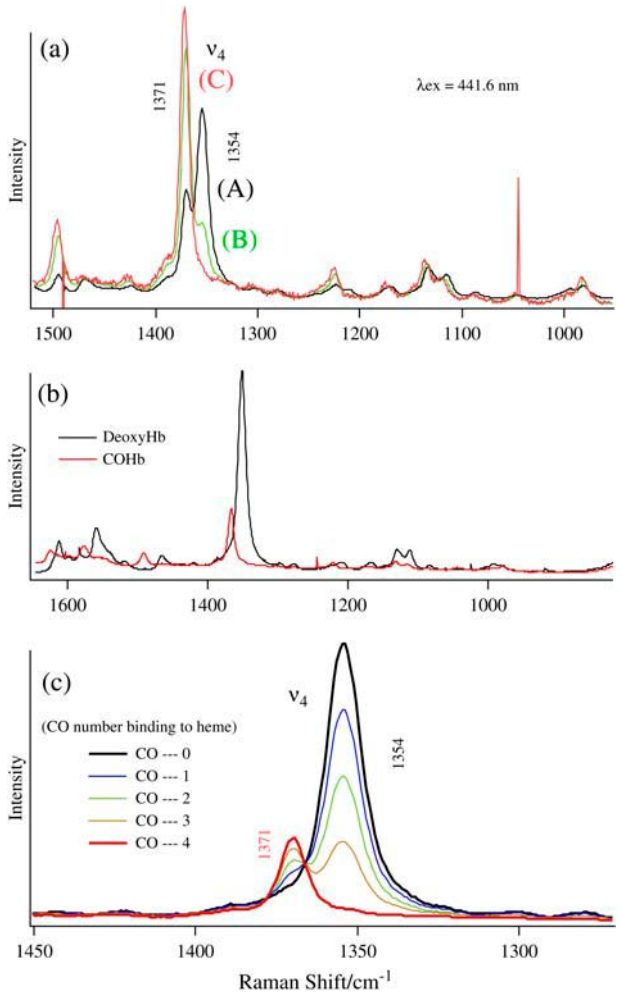

FIGURE 4 (a) The 441.6-nm excited RR spectra of COHb in a steady state at pH 6.6 with 1 mM BZF and 5 mM IHP, measured with a spinning cell of varied rates: (A) 1800 rpm; (B) 600 rpm; and (C) 180 rpm. Laser power used was 3.0, 0.37, and 0.027 mW for A, B, and C, respectively. (b) The 441.6-nm excited RR spectra of fully deoxyHbA and fully CO-bound HbA at pH 8.8 with no effector, measured with a spinning cell of 1800 rpm. The two spectra were observed under the same experimental conditions with a laser power of 110 μW at the sample point. All samples are equilibrated with 0.05 M HEPES buffer, containing 0.1 M Na_2SO_4, and protein concentrations were 200 μM in heme. (c) Simulated ν_4 bands for different numbers (m = 0–4) of CO molecules bound to Hb, which were calculated from the spectra shown in the middle panel.

Since it is well established that the ν_4 band appears at 1371 and 1354 cm^{-1} for CO- and deoxy-hemes, respectively, we can estimate a proportion of photodissociated hemes from the relative area intensity of the ν_4 bands. Fig. 4 a displays the spectra of COHb in solvent condition 5 observed with a spinning cell of varied rates and with different laser powers. Spectra A and C were obtained with the highest (3 mW) and the lowest (27 μW) laser powers, respectively. It is apparent that intensity of the 1354 cm^{-1} band (ν_4 band of photodissociated species) increases with increase of laser power at the expense of intensity of the 1371-cm^{-1} band (ν_4 band of CO-bound species). The intensities of 100% deoxyHb ($m = 0$) and 100% COHb ($m = 4$) excited at 441.6 nm with the experimental conditions described here are delineated in Fig. 4 b. Due to the closer proximity of the Raman excitation wavelength to the Soret band of the deoxy form than to that of the CO-form, the 1354-cm^{-1} band is much stronger than the 1371-cm^{-1} band. By combining the two spectra with an appropriate ratio, the expected spectra for a given m could be synthesized as shown by Fig. 4 c. Since the self-absorption effect on the band intensities was corrected by using the band intensity of SO_4^{2-} ion, the intensities of the ν_4 bands reflect the populations of each species. Accordingly, these curves were used as the calibration curves for determining m, that is, the extent of photodissociation under the laser power used. It is emphasized that m is determined in the same experiments as the determination of the $\nu_{\text{Fe-His}}$ frequency, although m is an average number.

Fig. 5 shows the 441.6-nm excited RR spectra of COHb observed with a spinning cell of variable rates. A rate of spinning was 1800, 600, and 180 rpm for spectra A, B, and C, respectively, and accordingly, the residence time of a given molecule in the laser beam was 1.3 (A), 4.0 (B), and 13 (C) ms. For spectra A–C shown in Fig. 5, m was adjusted to be 2.8 by changing a laser power under solvent condition 5 (containing 1 mM BZF and 5 mM IHP at pH 6.4). Spectrum D was observed for COHb for condition 1, that is, at pH 8.8 in the absence of any allosteric effectors with the same instrumental conditions as those used for spectrum C. The

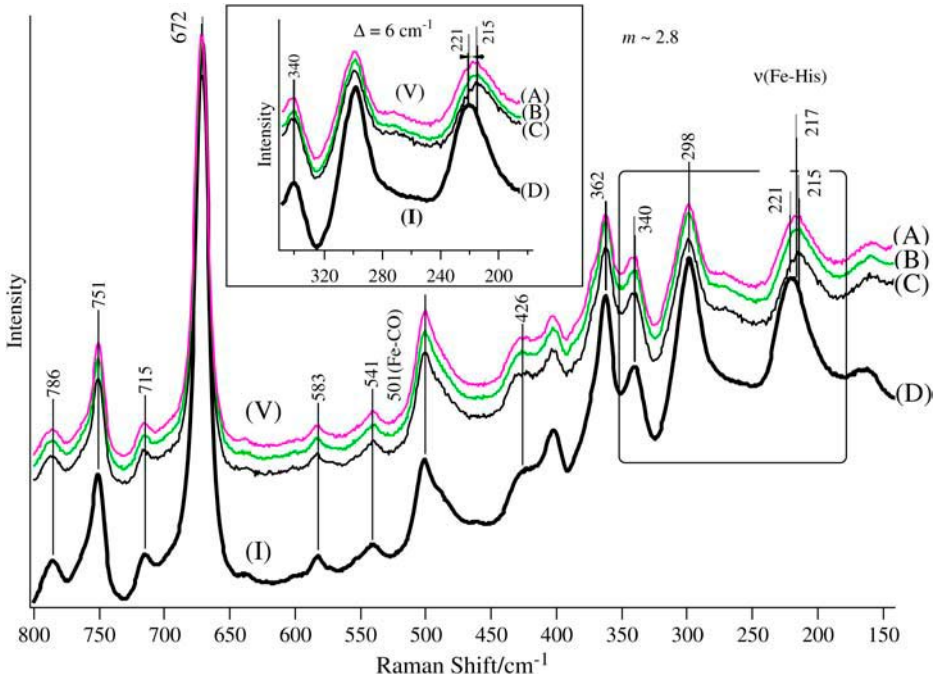

FIGURE 5 The 441.6-nm excited RR spectra of COHb for a certain fixed number of CO molecules bound to Hb under solution conditions 5 and 1. The spinning rate of the cell is 1800 rpm (*A*), 600 rpm (*B*), and 180 rpm (*C*) for solution 5 and 180 rpm for solution 1 (*D*). All samples are equilibrated with 0.05 M HEPES buffer, containing 0.1 M Na_2SO_4. Protein concentrations were 200 μM in heme.

overall spectral patterns of *A–D* are alike but the $\nu_{Fe\text{-}His}$ band position is slightly different; 217, 215, 215, and 221 cm^{-1} for spectra *A–D*, respectively. This part of the spectra is expanded in the inset with respect to the abscissa axis. The frequency of the γ_7 band at 298 cm^{-1} does not differ among the four spectra, but the band position of $\nu_{Fe\text{-}His}$ meaningfully differs among them.

Recalling that the $\nu_{Fe\text{-}His}$ frequency of transient deoxyHb at 10 ps after photolysis was 229–231 cm^{-1} in Fig. 2, $\nu_{Fe\text{-}His}$ frequencies *A–C* in Fig. 5 are fairly close to that of the equilibrium deoxyHb. Although the relaxation of the Fe-His bond may not be completely finished at 1.3 ms, it seems to be completed at 4.0 ms for solvent condition 5, because the frequencies for the delay times of 4.0 and 13 ms are identical. This observation serves as the experimental evidence for the presumption that three or more photons are not eventually involved in this measurement. If the recombined CO is photodissociated again by the third photon, the high-frequency $\nu_{Fe\text{-}His}$ band would have contributed to the spectrum. It is noted that the $\nu_{Fe\text{-}His}$ frequency at 13 ms after photolysis for solvent condition 1 is still higher than that of the stationary state (spectrum *D* in Fig. 1) and close to that of equilibrium deoxyHb in the R structure (36). This means that the magnitude of strain exerted on the Fe-His bond of deoxy subunits of COHb for $m = 2.8$ in solvent condition 1 is that of the R quaternary structure of equilibrium deoxyHb.

Fig. 6 displays typical RR spectra in the $\nu_{Fe\text{-}His}$ region observed under two different solvent conditions (1 and 5), with different laser powers but with a constant spinning rate. The simultaneously observed spectra in the ν_4 band are also delineated in the inset of individual panels. Panels *a* and *b* show the spectra observed for solvent conditions 1 and 5, respectively, which had been thought to adopt the normal R- and T-like quaternary state, respectively, in the CO-bound form. Since *m* is changed for the same residence time, possible time dependence of frequencies is removed from consideration.

In both panels of Fig. 6, the top spectra (*A* and *A′*) were obtained with the equilibrium deoxyHb for which the $\nu_{Fe\text{-}His}$ band is seen at 215 cm^{-1}. The behaviors of the $\nu_{Fe\text{-}His}$ frequency for intermediately ligated Hb are distinctly different between panels *a* and *b*. The $\nu_{Fe\text{-}His}$ frequency for solution 1 changes with *m* (231, 225, 224, 221, 220, 218, and 217 cm^{-1} for $m = 3.9$, 3.6, 3.3, 2.8, 2.1, 1.7, and 1.3) for a residence time of 13 ms. For solution 5, on the other hand, the $\nu_{Fe\text{-}His}$ band is absent for $m = 3.8$ but changes little with *m* when present: 215 and 215 cm^{-1} for $m = 3.5$ and 2.9. A shoulder might be present around 229 cm^{-1} in spectrum *C′*, and a very weak and broad feature seems to be present around 229 cm^{-1} in spectrum *D′*, which is close to the frequency detected for the 10-ps photoproduct (see Fig. 2). For both solutions, the intensity of the $\nu_{Fe\text{-}His}$ band increases as *m* becomes smaller.

The Fe-CO stretching mode ($\nu_{Fe\text{-}CO}$) at 500 cm^{-1} seems to exhibit broadening for smaller *m* values. This is caused by relatively increased contributions from the porphyrin band around 500 cm^{-1} upon weakening of the $\nu_{Fe\text{-}CO}$ band for smaller *m* numbers. The $C_\beta C_c C_d$ bending band of propionate side chains at 363 cm^{-1} becomes sharp when the $\nu_{Fe\text{-}His}$ band appears below 221 cm^{-1}. The $C_\beta C_a C_b$ bending modes of vinyl side chains around 424 and 405 cm^{-1} also exhibit a trend similar to that of the propionate band.

The frequency difference of $\nu_{Fe\text{-}His}$ for $m = 2.8$ at the residence time of 13 ms between solutions 1 and 5 shown in Fig. 5 are now confirmed in the independent measurements shown in Fig. 6; spectrum *E* in panel *a* and spectrum *B′* in

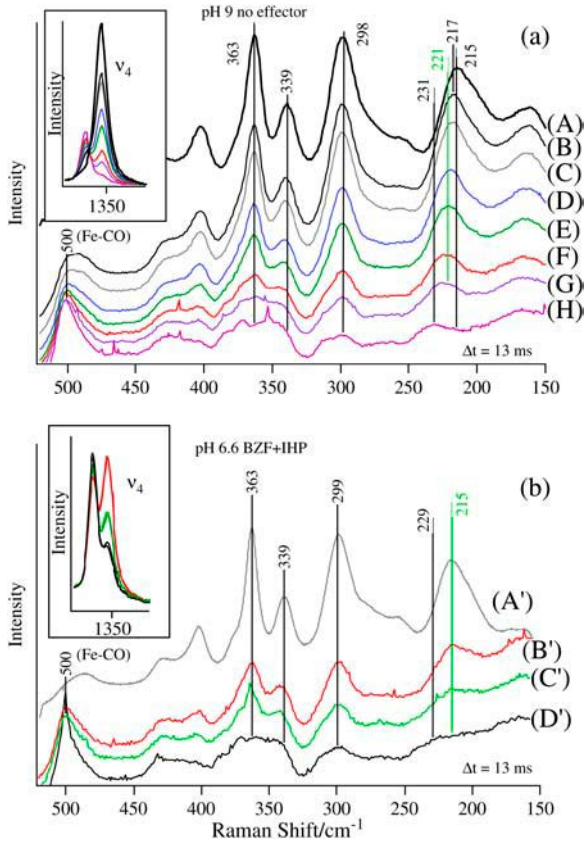

FIGURE 6 The 441.6-nm excited RR spectra of COHb in solution conditions 1 (*a*) and 5 (*b*) observed with different laser powers under constant spinning rate (180 rpm), except for *A* and *A′*, which represent the spectra of deoxyHb. The *m* value for each spectrum of solution 1 in panel *a* is as follows: 1.3 (*B*), 1.7 (*C*), 2.1 (*D*), 2.8 (*E*), 3.3 (*F*), 3.6 (*G*), and 3.9 (*H*). The *m* value of COHb for each spectrum in solution 5 in panel *b* in the presence of IHP and BZF at pH 6.6 is as follows: 2.9 (*B′*), 3.5 (*C′*), and 3.8 (*D′*). The *m* values were determined with the corresponding ν_4 spectra in the inset figures and the calibration curves shown in Fig. 4 *c*. All samples are equilibrated with 0.05 M HEPES buffer, containing 0.1 M Na_2SO_4. Protein concentrations were 200 μM in heme.

panel *b*. Since the $\nu_{\text{Fe-His}}$ band of deoxyHb in equilibrium generally appears around 214–216 cm^{-1} for the T state and 220–224 cm^{-1} for the R state, the results suggest that COHb for $m = 2.8$ adopts the R state in solution 1 but the T state in solution 5. It is stressed that the $\nu_{\text{Fe-His}}$ band for $m = 3.6$ in solution 1 is observed at 225 cm^{-1} in the R range but that for $m = 3.5$ in solution 5 is seen at 215 cm^{-1} in the T range. This means that the quaternary structure is definitely different between the two solutions for intermediately ligated forms. The difference becomes smaller as *m* becomes smaller.

DISCUSSION

Structural influences of allosteric effectors

Cooperativity and oxygen affinity of Hb A changes greatly with solution conditions including the presence and absence of an allosteric effector (7,41). Yonetani et al. found that simultaneous presence of BZF and IHP (or BPG) at pH 6.6 brought about such strong effects as to produce the low-affinity extreme with no apparent cooperativity (7). The binding site of an effector to Hb A is different between BZF (within the α chain) and IHP (and BPG), which stays between the two β chains. However, the visible RR spectra reflecting the heme structure and the UVRR spectra reflecting the globin structure of Hb A in the presence of these effectors are qualitatively categorized into a few distinct groups, that is, deoxy-T, deoxy-R, ligated-T, and ligated-R, although there are some distributions within a given group (17–22). The distribution in the T state was previously stressed as a plasticity by Friedman and co-workers (8), in consonance with this work. It is a premise that the $\nu_{\text{Fe-His}}$ frequency reflects the magnitude of strain exerted on the Fe-His bond and accordingly that some tertiary structure change is indispensable to change the $\nu_{\text{Fe-His}}$ frequency, but when the frequency change is correlated with a change of subunit contacts, the band is called a quaternary-structure marker for convenience. The visible RR spectra shown in Fig. 1, which are all deoxy-T type, indicate that allosteric effectors hardly influence the static structure of deoxy heme. It is emphasized that the low-affinity extreme, as seen for solution 5, does not generate stronger strain in the Fe-His bond.

The 10-ps transient RR spectra shown in Fig. 2, which were obtained for average 10% photodissociation of COHb but do not contain the contribution from the remaining COHb by spectral subtraction, are deduced to reflect the structure of the tetramer before CO-photodissociation, because the relaxation time of a quaternary structure is not so fast. Even for a monomer, COMb, the earliest tertiary-structure change of globin, inferred from the time-dependent frequency shift of the $\nu_{\text{Fe-His}}$ band, takes place with a time constant of 100 ps (26,27,31,32). The corresponding frequency shift due to the tertiary-structure change of Hb A occurs with a time constant of ~300 ps (33). The similarity of spectra among *A–D* in Fig. 2 implies that the heme structures of transient deoxyHb in the four different solution conditions are alike. This strongly suggests that the structures of COHb before photolysis in four different solution conditions similarly adopt the R structure.

The UVRR spectra shown in Fig. 3, which contain mainly the side-chain vibrations of aromatic residues, exhibit rather typical T-minus-R difference spectra for all four different solution conditions despite the fact that oxygen affinity and cooperativity are greatly different, as indicated in Table 1; Hill coefficients for conditions 1–5 are 2.5, 3.0, 2.1, 1.9, and 1.3. Cooperativity for condition 5 is almost nothing. It is worth noting that the deoxy-minus-CO differences of the isolated α and β chains gave no such difference peaks. The deoxy-minus-CO difference spectra observed for Hb A (Fig. 3) are different from that observed for the isolated α and β chains and also from those of Mb, which were definitely ascribed to a tertiary-structure change and ascribed to Tyr146 (sperm whale) and Trp7 (horse and sperm whale) (42). The

UVRR spectral differences between deoxyHb and COHb are ascribed to the changes of subunit contacts of Tyrα42, Tyrα140, Tyrβ145, and Trpβ37 (20,21), that is, quaternary structure changes. Thus, the UVRR spectral changes of globin due to the tertiary-structure change for the isolated α and β chains are distinguished from those due to the quaternary-structure change for Hb A.

These Raman results suggest that the structural differences of globin between fully deoxy- and fully CO-bound forms of Hb are hardly altered by the presence of allosteric effectors. This is consistent with the disappearance of the T marker band in the ^{1}H NMR spectrum that demonstrated the formation of the R quaternary structure for the fully ligated form of Hb A in the presence of IHP and BZF (7). Regarding UVRR spectra, the peak intensities in the deoxy-minus-CO difference spectra were slightly influenced by the presence of IHP and BZF as displayed in Fig. 3, whereas their spectral patterns are little altered. In contrast, appreciable effects appeared in the Fe-His stretching band in Fig. 6, which suggested that the influences of effectors would be present in the intermediately ligated forms ($m \neq 0$ or 4) rather than the initial ($m = 0$) and final ($m = 4$) states of ligand binding.

Fig. 5 shows the time dependence of photodissociated deoxyHb A in the simultaneous presence of BZF and IHP for a certain fixed number of CO molecules bound to Hb, which is 2.8 in this case. To keep m constant, a laser power was changed in the measurements for different periods of illumination time. The $\nu_{\text{Fe-His}}$ frequency is 217 cm^{-1} at $\Delta t = 1.3$ ms and 215 cm^{-1} at 13 ms. This frequency difference is much smaller than the difference (6 cm^{-1}) between the absence (221 cm^{-1}, D) and presence of BZF and IHP at the same Δt value (13 ms) for $m = 2.8$. The latter frequency difference is considered to represent the status difference of the Fe-His bond of the relaxed deoxy subunits of partially ligated tetramers between the two solution conditions; that is, it stays in the T-like and R-like states in solution conditions 5 and 1, respectively, because the structural relaxation has been almost finished in the millisecond time regime (8,9). It is noted that the Fe-CO stretching band is observed at 501 cm^{-1} in all spectra of Fig. 5. This means that the distal structure of globin in the ligated subunits is hardly altered in this time regime or by the presence of allosteric effectors. The structural influences of the effectors seem to appear most sensitively in the Fe-histidine (F8) bond.

Since the $\nu_{\text{Fe-His}}$ frequency at $\Delta t = 13$ ms is considered to represent the relaxed form, the differences in the $\nu_{\text{Fe-His}}$ frequencies shown in Fig. 6, obtained with a constant spinning rate ($\Delta t = 13$ ms) with different laser powers, would be attributed mainly to differences in m. Comparison of the two spectra in the upper and lower panels of Fig. 6 demonstrates that the $\nu_{\text{Fe-His}}$ frequency is distinctly lower in the presence of BZF and IHP for intermediately ligated forms, and that the difference is more noticeable for larger m values. This demonstrates that the quaternary structure of COHb in the presence of BZF and IHP adopts the T state insofar as only a small amount of CO is dissociated, but not always so, in their absence.

Provided that the Adair constants (K_i) (43) and partial pressure of ligands (p) are known, the fraction (f_i) of molecular species bound with i molecules of ligands is given by

$$f_i = g_i(p)/(1 + 4K_1p + 6K_1K_2p^2 + 4K_1K_2K_3p^3 + K_1K_2K_3K_4p^4),$$

where $g_0(p) = 1$, $g_1(p) = 4K_1p$, $g_2(p) = 6K_1K_2p^2$, $g_3(p) = 4K_1K_2K_3p^3$, and $g_4(p) = K_1K_2K_3K_4p^4$ (43,44). We tentatively assumed the K values of stripped Hb at pH 9 ($K_1 = 4.46 \times 10^{-4}$ Pa^{-1} ($= 0.0595$ mmHg^{-1}), $K_2 = 1.2 \times 10^{-3}$ ($= 0.16$), $K_3 = 1.1 \times 10^{-2}$ ($= 1.5$), and $K_4 = 2.50 \times 10^{-2}$ ($= 3.33$)) for condition 1 and used the reported values ($K_1 = 4.73 \times 10^{-5}$ Pa^{-1} ($= 0.00630$ mmHg^{-1}), $K_2 = 6.83 \times 10^{-5}$ ($= 0.00910$), $K_3 = 8.63 \times 10^{-5}$ ($= 0.0115$), and $K_4 = 1.34 \times 10^{-4}$ ($= 0.0179$)) for condition 5. For suitably selected values of p and f_i, the m values, which corresponds to $\Sigma i \times f_i$, were calculated as shown in Table 2. Since the effective partial pressure of CO (p) in the photo-steady-state is different from the experimental value, only the differences in distribution of f_i between the two different solution conditions are significant in Table 2.

For solution condition 1, the $\nu_{\text{Fe-His}}$ frequency is 225 cm^{-1} for $m = 3.6$ and 220 cm^{-1} for $m = 2.1$. The former and latter are predominantly ascribed to the species with three ligands (f_3) and the fully deoxy species (f_0), respectively. These

TABLE 2 Distributions of intermediately ligated hemoglobins for selected values of partial pressure of oxygen calculated with the assumed values of Adair constants

Solution	p/Pa	f_0	f_1	f_2	f_3	f_4	$\Sigma i \times f_i$	Spectrum	(m value)
1-Like	1.81×10^3	0	0	0	0.10	0.90	3.9	H	3.9
	6.97×10^2	0.03	0.03	0.03	0.16	0.75	3.6	G	3.6
	3.89×10^2	0.15	0.10	0.05	0.20	0.50	2.8	E	2.8
	2.94×10^2	0.28	0.16	0.05	0.19	0.32	2.1	D	2.1
5-Like	1.53×10^5	0	0	0.02	0.16	0.82	3.8	D′	3.8
	6.21×10^4	0	0.01	0.08	0.29	0.61	3.5	C′	3.5
	2.76×10^4	0.02	0.08	0.22	0.36	0.33	2.9	B′	2.9

Adair constants of $K_1 = 4.46 \times 10^{-4}$, $K_2 = 1.2 \times 10^{-3}$, $K_3 = 1.1 \times 10^{-2}$, and $K_4 = 2.50 \times 10^{-2}$ Pa^{-1}, similar to the case of stripped Hb at pH 9 (41), were assumed for the 1-like condition and constants of $K_1 = 4.73 \times 10^{-5}$, $K_2 = 6.83 \times 10^{-5}$, $K_3 = 8.63 \times 10^{-5}$, and $K_4 = 1.34 \times 10^{-4}$ Pa^{-1}, as obtained for solution 5 (7), were used for the 5-like condition.

frequencies belong to the category of the R type deoxyHb (36). For solution condition 5, however, the $\nu_{\text{Fe-His}}$ frequency is 215 cm^{-1} for $m = 3.5$ and 2.9 and the main contributor to this band is the species with three ligands (f_3). This frequency belongs to the category of T-type deoxyHb. In spectrum D', there might be a weak peak around 229 cm^{-1} and an origin of this band, if present, is the species with three ligands (f_3). This may suggest to us that the T and R structures are coexistent for $m = 3.8$ but the T structure gains in strength upon decrease to $m = 3.5$ and becomes dominant for $m = 2.9$. In other words, the dependence of T and R populations on m is distinctly different between solutions 5 and 1; it is mainly T for $m \leq 3.5$ in the presence of BZF and IHP (solution 5) but is R even for $m = 2.1$ in the absence of any effectors (solution 1).

In the case of solution 1, the $\nu_{\text{Fe-His}}$ frequencies 218 and 217 cm^{-1} for $m = 1.7$ and $m = 1.3$, respectively, are considered to arise from the fully deoxy (f_0) species and the species with one (f_1) or three (f_3) ligands according to the calculation, representing that the deoxy subunit of the partially ligated tetramer adopts the T structure, though not to the same extent as 215 cm^{-1} of fully deoxyHb as a whole molecule. Although the f_0 contribution is dominant (f_0, 38% for $m = 1.7$, and f_0, 48% for $m = 1.3$), the contribution from f_3 is as large as 10–15%. If the f_3 portion gives the $\nu_{\text{Fe-His}}$ band at ~223 cm^{-1} like R-type deoxyHb A, without being resolved from the contribution from the f_0 and f_1 portions at 215 cm^{-1}, the peak position of the composite band would be shifted to 217 cm^{-1}. This was confirmed by simulation using Gaussian band-shape functions. Even if it is not the case, it would simply mean that a deoxy subunit in the f_3 portion takes a T-like, but not the typical T, structure. In other words, their tertiary structures are somewhat different depending on m, even though the subunit contact (and the magnitude of strain in globin) belongs to the category of the T type. This corresponds to the subsets of T in the notation of Friedman and co-workers (8). In this regard, the T/R two-state model is not sufficient to explain the results described here. In other words, the T structure for $m = 0$ and that for $m = 2$ would be different albeit the same ''T'' is used.

Relation between cooperativity and oxygen affinity

One of the effects of allosteric effectors of Hb A is to decrease oxygen affinity (7). A binding scheme of effector molecules to Hb is not always universal, but their binding decreases the oxygen affinity for the deoxy form more than for partially ligated forms. As a result, the Hill coefficient changes sensitively with effectors. The simultaneous presence of IHP and BZF lowers the oxygen affinity of both the deoxy and ligated forms, and as a result, the Hill coefficient is almost at unity. This feature may indicate that the T-to-R quaternary-structure change does not take place upon oxygen binding, and that only the tertiary structure changes (16). However, the ^{1}H NMR study demonstrated a change of spectral pattern to that of the R structure for the fully ligated Hb in the presence of BZF and IHP (7). Our Raman results are compatible with the ^{1}H NMR results. The protein contacts at subunit interfaces, as well as the heme structure for complete deoxyHb, were not altered by the presence of IHP, BPG, or BZF. They are of ordinary T type. On the other hand, the contacts of residues in the subunit interface, as well as the heme structure of the fully ligated form, which were distinct from those of deoxyHb, were also hardly influenced by the presence of IHP, BPG, or BZF. Judging from the $\nu_{\text{Fe-His}}$ frequency, the T-to-R transition takes place when the average m of bound ligands is 3.5 in the presence of BZF and IHP but <2.1 in the absence of any allosteric effectors. Since the binding of allosteric effectors affects the quaternary structure of intermediately ligated forms, the switching m seems to depend on the molecular species of effectors. It is considered that structural relaxation has almost been finished at 13 ms after CO photolysis and, therefore, the $\nu_{\text{Fe-His}}$ frequency at $\Delta t = 13$ ms shown in Fig. 6 *b* would reflect the equilibrium structure of the intermediately ligated form in the presence of IHP and BZF at pH 6.6.

Our results can satisfactorily be interpreted within the category of the two-state model, as illustrated in Fig. 7, where free energy levels for T_m and R_m are schematically drawn. Here, ΔG_T and ΔG_R represent the free energy decrease upon binding of a ligand within the T and R quaternary structures, respectively, and the subscript m denotes the m value, which is the number of ligand molecules bound to Hb. It is assumed that solution conditions change the energy of the T system relative to that of the R system. If the T_3 level is significantly higher than the R_3 level, as indicated by black lines, the quaternary transition is expected to occur in the intermediate state around $m = 2$–3, and cooperativity would be observed for ligand binding. This corresponds to solution condition 1. In contrast, if the T_3 level is lower than the R_3 level and T_4 is higher than R_4, as indicated by shaded lines, the quaternary structure change occurs upon binding of the fourth ligand, and in this case cooperativity would not be apparently observed for ligand binding. Since ΔG for the last step (ΔG_R) would be slightly larger than other ΔG (ΔG_T), the binding constant would increase in the final stage of ligand binding, but the affinity for ligand would remain low until the final stage of ligand binding. This means that cooperativity is apparently lost despite the fact that the fully ligated form adopts the R structure. In this case T_4 might be coexistent with R_4 in equilibrium. Presumably this corresponds to solution condition 5 of our study. This interpretation is incompatible with the theory that the quaternary structure transition occurs between T_2 and R_3 in the presence of BZF and IHP at pH 6.6 (7), and in fact, there is no experimental evidence for the presence of R_3. On the contrary, this study demonstrated that the presence of T_3, that is, Hb in solution condition 5 mainly adopts the T structure at $m = 3.5$.

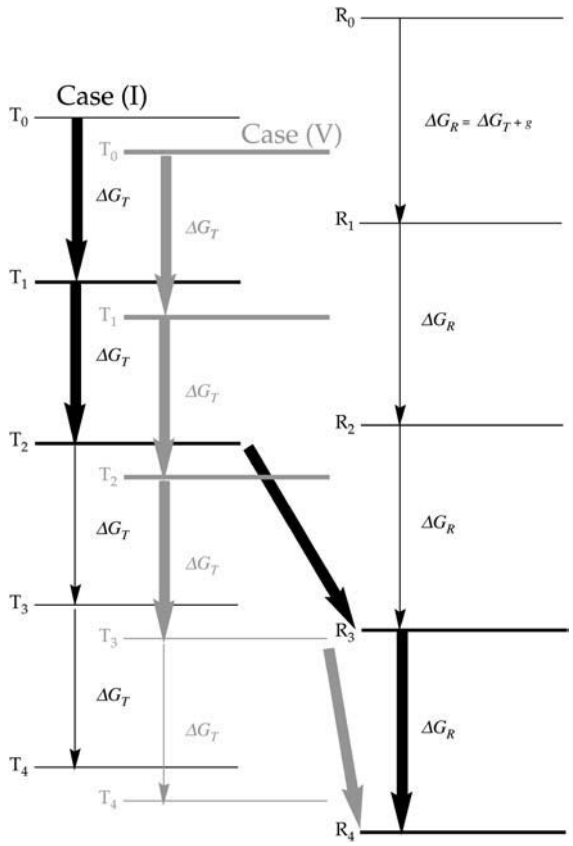

FIGURE 7 Schematic free energy diagram of Hb for oxygen binding. Gibbs free energy level of T_0–T_4 and R_0–R_4 are represented by horizontal bars, in which subscripts denote the *m* value. It is assumed that the T_0–T_4 system is changed relative to the R_0–R_4 system from black to gray by the change of solvent conditions from 1 to 5. When T_3 is higher than R_3 (*black lines*), the intersystem crossing occurs in the T_2-to-R_3 transition. When T_3 is lower than R_3 (*shaded lines*), the intersystem switching occurs between T_3 and R_4, and as a result, cooperativity is apparently lost.

Our conclusion in this work is consistent with the observations for Hb Kansas (β102Asn → Thr). The T-to-R switching point of Hb Kansas is thought to be 3.5, in contrast with 2.5 for Hb A (6), and the UVRR difference spectrum between deoxy and fully CO-bound states of Hb Kansas exhibited a pattern quite similar to that of the ordinary T-minus-R difference (Fig. 3, spectrum *E*), although peak intensities were appreciably weaker (M. Nagai, unpublished data). The origin of the weaker difference intensity is ascribed to the CO-bound form, because deoxyHb Kansas minus deoxyHb A exhibited almost nothing, but COHb Kansas minus COHb A gave weak positive peaks, the pattern of which was close to that of the T-minus-R difference spectrum. This means that COHb Kansas contains a small amount of T species even after complete CO binding on account of proximity of free energies of T_4 and R_4, and the subunit contacts in such molecules are kept in the T type despite the ligated form. Thus, Hb in solution condition 5 is considered to be close to Hb Kansas, with larger T_4/R_4 energy separation for the former than for the latter.

This work was supported by a Grant-in-Aid for Specifically Promoted Research to T.K. (14001004) from the Ministry of Education, Sports, Culture, Science and Technology, Japan, Grant-in-Aid for Scientific Research (C) from Japan Society for Promotion of Science to M.N. (14570103), and Research Grant from the National Heart, Lung, and Blood Institute, National Institutes of Health, to T.Y. (HL14508).

REFERENCES

1. Monod, J., J. Wyman, and J. P. Changeux. 1965. On the nature of allosteric transition: a plausible model. *J. Mol. Biol.* 12:88–118.
2. Perutz, M. F. 1970. Stereochemistry of cooperative effects in haemoglobin. *Nature*. 228:726–739.
3. Perutz, M. F. 1979. Regulation of oxygen affinity of hemoglobin: influence of structure of the globin on the heme iron. *Annu. Rev. Biochem.* 48:327–386.
4. Perutz, M. F., G. Fermi, B. Luisi, B. Shaanan, and R. C. Liddington. 1987. Stereochemistry of cooperative mechanisms in hemoglobin. *Acc. Chem. Res.* 20:309–321.
5. Perutz, M. F. 1990. Mechanisms regulating the reactions of human hemoglobin with oxygen and carbon monoxide. *Annu. Rev. Physiol.* 52:1–25.
6. Shulman, R. G., J. J. Hopfield, and S. Ogawa. 1975. Allosteric interpretation of haemoglobin properties. *Q. Rev. Biophys.* 8: 325–420.
7. Yonetani, T., S. I. Park, A. Tsuneshige, K. Imai, and K. Kanaori. 2002. Global allostery model of hemoglobin. Modulation of O_2 affinity, cooperativity, and Bohr effect by heterotropic allosteric effectors. *J. Biol. Chem.* 277:34508–34520.
8. Samuni, U., L. Juszczak, D. Dantsker, I. Khan, A. J. Friedman, J. Perez-Gonzalez-de-Apodaca, S. Bruno, H. L. Hui, J. E. Colby, E. Karasik, L. D. Kwiatkowski, A. Mozzarelli, R. Noble, and J. M. Friedman. 2003. Functional and spectroscopic characterization of half-liganded iron-Zinc hybrid hemoglobin: evidence for conformational plasticity within the T state. *Biochemistry*. 42:8272–8288.
9. Peterson, E. S., R. Shinder, I. Khan, L. Juczszak, J. Wang, B. Manjula, S. A. Acharya, C. Bonaventura, and J. M. Friedman. 2004. Domain-specific effector interactions within the central cavity of human adult hemoglobin in solution and in porous sol-gel matrices: Evidence for long-range communication pathways. *Biochemistry*. 43: 4832–4843.
10. Arnone, A. 1972. X-ray diffraction study of binding of 2,3-diphosphoglycerate to human deoxyhaemoglobin. *Nature*. 237:146–149.
11. Benesch, R., and R. E. Benesch. 1967. The effect of organic phosphates from the human erythrocyte on the allosteric properties of hemoglobin. *Biochem. Biophys. Res. Commun.* 26:162–167.
12. Perutz, M. F., and C. Poyart. 1983. Bezafibrate lowers oxygen affinity of haemoglobin. *Lancet*. 2:881–882.
13. Baldwin, J., and C. Chothia. 1979. Haemoglobin: the structural changes related to ligand binding and its allosteric mechanism. *J. Mol. Biol.* 129:175–220.
14. Fung, L. W.-M., and C. Ho. 1975. Proton nuclear magnetic resonance study of the quaternary structure of human hemoglobins in water. *Biochemistry*. 14:2526–2535.
15. Ho, C. 1992. Proton nuclear magnetic resonance studies on hemoglobin: cooperative interactions and partially ligated intermediates. *Adv. Protein Chem.* 43:192–214.
16. Shibayama, N., S. Miura, R. H. J. Tame, T. Yonetani, and S.-Y. Park. 2002. Crystal structure of horse carbonmonoxyhemoglobin-bezafibrate complex at 1.55-Å resolution. A novel allosteric binding site in R-state hemoglobin. *J. Biol. Chem.* 277:38791–38796.
17. Kitagawa, T. 1988. Biological applications of raman spectroscopy. *In* Biological Applications of Raman Spectroscopy, Vol. 3. T. G. Spiro, editor. John Wiley & Sons, New York. 97–131.

18. Hu, X., K. R. Rodgers, I. Mukerji, and T. G. Spiro. 1999. New light on allostery: dynamic resonance Raman spectroscopy of hemoglobin Kempsey. *Biochemistry.* 38:3462–3467.

19. Rodgers, K. R., and T. G. Spiro. 1994. Nanosecond dynamics of the R→T transition in hemoglobin: ultraviolet Raman studies. *Science.* 265:1697–1699.

20. Nagai, M., S. Kaminaka, Y. Ohba, Y. Nagai, Y. Mizutani, and T. Kitagawa. 1995. Ultraviolet resonance Raman studies of quaternary structure of hemoglobin using a tryptophan β37 mutant. *J. Biol. Chem.* 270:1636–1642.

21. Nagai, M., H. Wajcman, A. Lahary, T. Nakatsukasa, S. Nagatomo, and T. Kitagawa. 1999. Quaternary structure sensitive tyrosine residues in human hemoglobin: UV resonance Raman studies of mutants at α140, α35, and β145 tyrosine. *Biochemistry.* 38:1243–1251.

22. Nagai, M., M. Nishibu, Y. Sugita, Y. Yoneyama, R. T. Jones, and S. Gordon. 1975. The effects of inositol hexaphosphate on the allosteric properties of two beta-99-substituted abnormal hemoglobins, hemoglobin Yakima and hemoglobin Kempsey. *J. Biol. Chem.* 250: 3169–3173.

23. Kaminaka, S., and T. Kitagawa. 1995. Novel spinning cell system for UVRR measurements of powder and small-volume solution samples in back-scattering geometry: application to solid tryptophan and mutant hemoglobin solution. *Appl. Spectrosc.* 49:685–687.

24. Ogura, T., S. Takahashi, S. Hirota, K. Shinzawa-Itoh, S. Yoshikawa, E. Appelman, and T. Kitagawa. 1993. Time-resolved resonance Raman elucidation of the pathway for dioxygen reduction by cytochrome c oxidase. *J. Am. Chem. Soc.* 115:8527–8536.

25. Kaminaka, S., and T. Kitagawa. 1992. A novel idea for practical UV resonance Raman measurement with a double monochromator and its application to protein structural studies. *Appl. Spectrosc.* 4:1804–1808.

26. Mizutani, Y., and T. Kitagawa. 2001. Ultrafast dynamics of myoglobin probed by time-resolved resonance Raman spectroscopy. *Chem. Rec.* 1:258–275.

27. Mizutani, Y., and T. Kitagawa. 2001. Ultrafast structural relaxation of myoglobin following photodissociation of carbon monoxide probed by time-resolved resonance Raman spectroscopy. *J. Phys. Chem. B.* 105:10992–10999.

28. Uesugi, Y., Y. Mizutani, and T. Kitagawa. 1997. Developments of widely tunable light sources for picosecond time-resolved resonance Raman spectroscopy. *Rev. Sci. Instrum.* 68:4001–4008.

29. Hu, S., I. K. Morris, J. P. Singh, K. M. Smith, and T. G. Spiro. 1993. Complete assignment of cytochrome c resonance Raman spectra via enzymic reconstitution with isotopically labeled hemes. *J. Am. Chem. Soc.* 115:12446–12458.

30. Hu, S., K. M. Smith, and T. G. Spiro. 1996. Assignment of protoheme resonance Raman spectrum by heme labeling in myoglobin. *J. Am. Chem. Soc.* 118:12638–12646.

31. Lim, M., T. A. Jackson, and P. A. Anfinrud. 1993. Nonexponential protein relaxation: dynamics of conformational change in myoglobin. *Proc. Natl. Acad. Sci. USA.* 90:5801–5804.

32. Kuczera, K., J.-C. Lambry, J.-L. Martin, and M. Karplus. 1993. Nonexponential relaxation after ligand dissociation from myoglobin: a molecular dynamics simulation. *Proc. Natl. Acad. Sci. USA.* 90: 5805–5807.

33. Mizutani, M., B. Pal, M. Nagai, and T. Kitagawa. *In* Proceedings of the Eleventh International Conference on Time-resolved Vibrational Spectroscopy. In press.

34. Friedman, J. M., D. L. Rousseau, M. R. Ondrias, and R. A. Stepnoski. 1982. Transient Raman study of hemoglobin: structural dependence of the iron-histidine linkage. *Science.* 218:1244–1246.

35. Friedman, J. M., D. L. Rousseau, and M. R. Ondrias. 1982. Time-resolved resonance Raman studies of hemoglobin. *Annu. Rev. Phys. Chem.* 33:471–491.

36. Nagai, K., T. Kitagawa, and H. Morimoto. 1980. Quaternary structures and low frequency molecular vibrations of haems of deoxy and oxy-haemoglobin studied by resonance Raman scattering. *J. Mol. Biol.* 136: 271–289.

37. Harada, I., and H. Takeuchi. 1986. Raman and ultraviolet resonance raman spectra of proteins and related compounds. *In* Spectroscopy of Biological Systems. R. J. H. Clark and R. E. Hester, editors. John, Wiley & Sons, New York. 113–175.

38. Nagai, M., M. Aki, R. Li, Y. Jin, H. Sakai, S. Nagatomo, and T. Kitagawa. 2000. Heme structure of hemoglobin M Iwate [α87(F8)His → Tyr]: a UV and visible resonance Raman study. *Biochemistry.* 39:13093–13105.

39. Nagatomo, S., M. Nagai, A. Tsuneshige, T. Yonetani, and T. Kitagawa. 1999. UV resonance Raman studies of α-nitrosyl hemoglobin derivatives: relation between the α1-β2 subunit interface interactions and the Fe-histidine bonding of α heme. *Biochemistry.* 38:9659–9666.

40. Nagatomo, S., M. Nagai, N. Shibayama, and T. Kitagawa. 2002. Differences in changes of the α1-β2 subunit contacts between ligand binding to the α and β subunits of hemoglobin A: UV resonance Raman analysis using Ni-Fe hybrid. *Biochemistry.* 41: 10010–10020.

41. Imai, K. 1982. Allosteric Effects in Haemoglobin. Cambridge University Press, Cambridge, UK.

42. Haruta, N., M. Aki, S. Ozaki, Y. Watanabe, and T. Kitagawa. 2001. Protein conformation change of myoglobin upon ligand binding probed by ultraviolet resonance Raman spectroscopy. *Biochemistry.* 40:6956–6963.

43. Adair, G. S. 1925. The hemoglobin system. VI. The oxygen dissociation curve of hemoglobin. *J. Biol. Chem.* 63:529–545.

44. Wyman, J. 1967. Allosteric linkage. *J. Am. Chem. Soc.* 89:2202–2218.